



Proceeding Paper

Enhancing Fire Alarm Systems Using Edge Machine Learning for Smoke Classification and False Alarm Reduction [†]

Abdulrhman Alshaya * and Abdullah Almutairi

King Abdulaziz City for Science and Technology (KACST), Riyadh 12354, Saudi Arabia; amaalmutairi@kacst.gov.sa

- * Correspondence: aaalshaya@kacst.gov.sa
- [†] Presented at the 12th International Electronic Conference on Sensors and Applications (ECSA-12), 12–14 November 2025; Available online: https://sciforum.net/event/ECSA-12.

Abstract

A Traditional fire alarm systems use smoke sensors to monitor the concentration of smoke particles in the air. If the concentration exceeds a certain threshold, an alarm signal is triggered. However, this detection process could lead to false fire alarms, causing unnecessary evacuations and panic among residents. False alarms may result from activities such as smoking in non-smoking areas, burning Oud, or cooking smoke. In this study, a deep neural network (DNN) model was trained to classify three types of smokes that were Oud, Cigarette, and burning tissue smokes. The offline prediction accuracy of this model was 97.5%. The size of the model after converting it to TensorFlow lite was 4.7 Kbytes. It can be also converted to tiny model to deploy it on microcontroller.

Keywords: machine learning; gas classification; tiny-ML; edge computing; deep neural network

1. Introduction

The traditional fire alarm systems are essential components of an indoor safety environment. These systems typically rely on smoke sensors that set on an alarm if the concentration of smoke particles exceeds a specific threshold [1]. The downside of a similar system is unable to classify gasses and smokes which could lead to generate false alarms from non-threatening activities, such as Oud, Cigarette Smokes, or Cooking. These false alarms can cause panic, unnecessary evacuations, and a decline in trust in the reliability of fire alarm systems. By adding gasses and smokes classification, the system will be able to distinguish between hazardous and harmless smoke which will result in increasing the level of reliability on the system. Several studies have explore different mechanism to detect and classify leakage in different applications. For inctance, Barkani et al. [2] have deployed lightweight convolutional neural network on a microcontroller integrated with a thermal camera to detect gas leaks. Khan [3] have detected gas leakage based on the gas concentation using semiconductor sensors. Pan et al. [4] have utilized neural network, IoT technology, and surveillance camera to early detect fires. Sharma et al. [5] have inverstigated multiple gas sensors with thermal camera and federated learning tecchnique to detect gas leakages. However, there is no study classify different type of smokes in indoor environment that assists to enhance the performene of fire alarm system. Therefore, in this study, A deep neural network (DNN) was utilized to classify three different types of

Academic Editor(s): Name

Published: date

Citation: Alshaya, A.; Almutairi, A. Enhancing Fire Alarm Systems Using Edge Machine Learning for Smoke Classification and False Alarm Reduction. *Eng. Proc.* **2025**, *volume number*, x. https://doi.org/10.3390/xxxxx

Copyright: © 2025 by the authors. Submitted for possible open access publication under the terms and conditions of the Creative Commons Attribution (CC BY) license (https://creativecommons.org/license s/by/4.0/).

smokes, that were Cigarettes, Oud, and burning tissue smokes including fresh air (background) in indoor environment. The smoke classification DNN model can be converted to smaller model that can be deployed on microcontroller to enhance the performce of fire alarm detector. This classification process will provide users with a predicted smoke type before fire alarm.

2. Materials and Methods

2.1. System Description

In this study, Tiny-ML will be used to classify the source of smoke in indoor environment. The datasets that were used to train the machine learning model were acquired by using three different sensor modules as shown in Table 1 [6–12]. The first module (BME 680) was used to detect and measure volatile organic compounds (VOC), temperature, and humidity. The second sensor module (Grove–Multichannel Gas sensor V2) that consists of four gas sensors was utilized to detect carbon monoxide (CO), nitrogen dioxide (NO2), ethanol (C2H5CH), and volatile organic compounds (VOC). The third sensor module (MQ 136) acquired hydrogen sulfide. These sensor modules were integrated with Wio terminal microcontroller as shown in Figure 1. This Wio terminal was used because that it has ARM Cortex-M4F core running at 120 MHz. This microcontroller is also supporting Arduino library for tensorflow lite for microcontroller. Moreover, it has 4 MB external flash and 192 KB RAM. It is also supporting all communication protocol used by sensor modules. These features allow to deploying Tiny-ML model on it [13,14].

Table 1. Gas sensors Specifications.

Sensor		Target Gases	Detection Ranges
		Volatile Organic Compounds	VOCs (IAQ) = 0 to 500
BME 680		(VOCs), Temperature, and Hu-	Temperature (CO) = -40 to 85
		midity	Humidity (%) = 0 to 100
Grove-Multichannel			
Gas sensor V2			NO2(PPM) = 0.1 to 10
•	GM-102B	NO2 gas, Ethanol vapor, VOC	Ethanol (PPM) = $1 \text{ to } 500$
•	GM-302B	gas, and CO gas	VOC (PPM) = 1 to 500
•	GM-502B		CO(PPM) = 5 to 5000
•	GM-702B		
MQ 136		Hydrogen Sulfide (SnO2) gas	SnO2(PPM) = 1 to 200

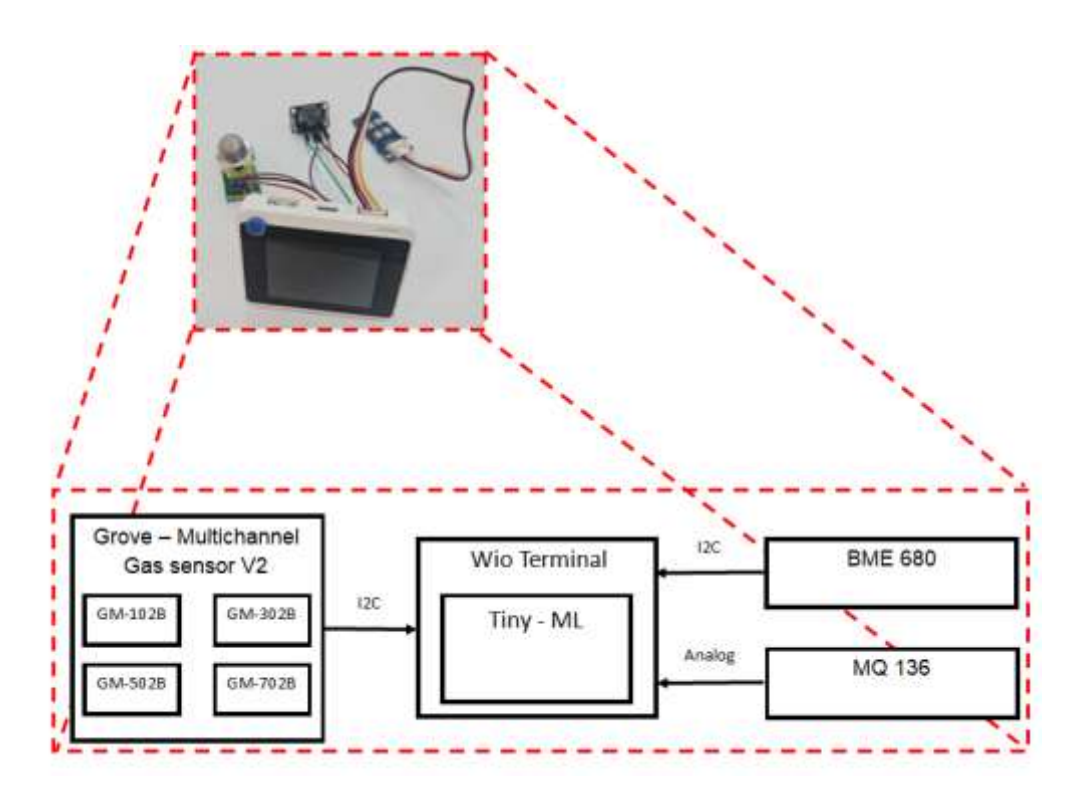


Figure 1. The Block diagram of the Fire alarm detector.

2.2. Data Collection and Calibration

Three types of smoke were used to collect datasets that were cigarettes, Oud, and burning tissue smokes including fresh air (background) in indoor environment. The size of the room that was used to collect datasets is around 76 m³. Moreover, the distance between the source of smoke and gas sensors was 30 cm. Before collecting smoke data, the used gas sensors were run for 48 h as preheat that is recommended in their datasheet [6–12]. After that, when these sensors were run again, they need almost 30 min as a preheat until the sensor data become stable. The smokes datasets were collected using Arduino and python code that were written by Shawn Hymel [15]. However, the Arduino code was modified to be suitable for collecting data from the used gas sensors. The sampling rate for these sensors were set to be 10 samples per second. 20 samples were also acquired for each single data file. These data files were saved in .CSV format. 2400 data files were collected for all smoke types including fresh air.

In this study, the output data from the gas sensors were affected by the temperature and humidity of the surrounding environment. Therefore, the collected dataset should be calibrated before using them in training Deep Neural Network (DNN) model. However, there is not clear equation or graph describe the relation between the output of these gas sensors and the temperature and humidity of the surrounding environment. To deal with this issue, the effect of changing surrounding temperature on the output of gas sensor was analyzed when the surrounding humidity was assumed fixed. This was done by acquiring data from gas sensors for a fresh air inside the room for different temperature values as shown in Figure 2. During the collection data, the humidity inside the room changed between 21% and 25%.

From Figure 2, it can be noticed that the output of GM-502B, GM-102B, and GM-302B sensors linearly increased when the room temperature increased (Figure 2A–C). When the room temperature increases from 22 °C to 26 °C, the output of GM-502B, GM-102B, and GM-302B sensors rise by 37, 47, and 45 a.u. respectively. The output of GM-702B slightly raised by changing the room temperature as shown in Figure 2D. The output of GM-702B increased by 5 a.u. when the room temperature change from 22 °C to 26 °C. The output of

MQ-136 sensor is almost not affected by temperature of the room as shown in Figure 2E. This led to neglect the effect of temperature on the output of MQ-136 sensor. In addition, the output of BME-860 VOC gas sensor reduced when the temperature of the surrounding environment increased as shown in Figure 2F. When the room temperature rise from 22 $^{\circ}$ C to 26 $^{\circ}$ C, the output of BME-860 VOC gas sensor reduced by 357.337 a.u.

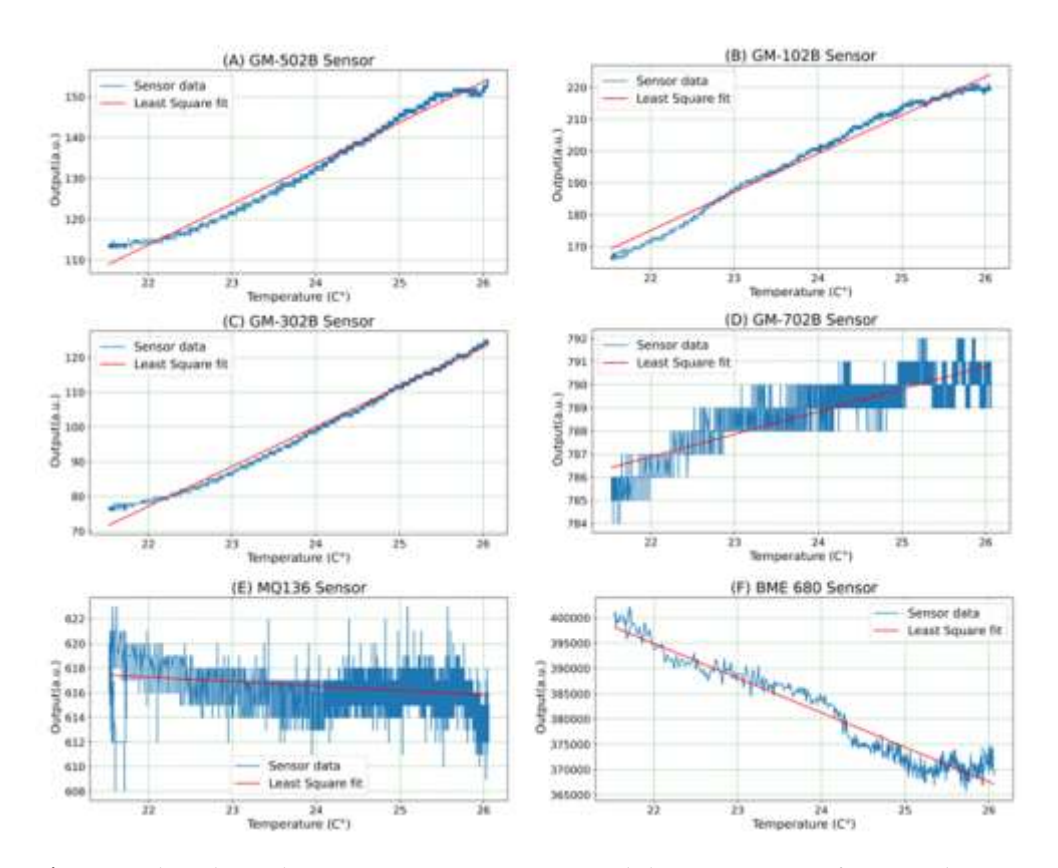


Figure 2. The relation between gas sensors output and the temperature of surrounding environment.

The least square method was used to determine the linear relation between the gas sensors outputs and temperature of the surrounding environment. Based on this method, the slope and y intercept for straight line Equation (1) were calculated [16].

$$Y = mX + b \tag{1}$$

where Y is the output of gas sensor, m is the slope, X is the temperature, and b is the y intercept. The slope (m) can be calculated by using Equation (2) [16]:

$$m = \frac{n\sum x_i y_i - \sum x_i \sum y_i}{n\sum x_i^2 - (\sum x_i)^2}$$
 (2)

where n is the number of samples. The y intercept (b) can be calculated using Equation (3) [16]:

$$b = \frac{\sum x_i^2 \sum y_i - \sum x_i \sum x_i y_i}{n \sum x_i^2 - (\sum x_i)^2}$$
(3)

The correlation between the output of gas sensors and the room temperature can be measure using Pearson Correlation Coefficient (r) as shown in Equation (4) [16]:

$$r = \frac{n\sum x_i y_i - \sum x_i \sum y_i}{\sqrt{(n\sum x_i^2 - (\sum x_i)^2)(n\sum y_i^2 - (\sum y_i)^2)}}$$
(4)

Based on these equations, the least square fitting functions and correlation coefficients between gas sensors outputs and temperature were calculating as shown in Table 2. There are high positive correlations (r = 0.99) between the output of GM-502B, GM-102B, and GM-302B gas sensors and room temperature. The output of GM-702B gas sensor has also high positive coefficient with room temperature that is 0.85. Whereas the output of MQ-136 sensor is not correlation with room temperature. The correlation coefficient between them is -0.29. In addition, the output of BME-860 VOC gas sensor has high negative correlation with the room temperature. It had -0.95 correlation coefficient. This means when the room temperature increase, the output of the gas sensor reduces. The least square fitting functions in Table 2 were used to plot the least square fitting straight line for each gas sensor in Figure 2.

Table 2. The least square fitting function and correlation coefficient between gas sensors outputs and surrounding environment temperature.

Gas Sensor	Least Square Fitting Function	Correlation Coefficient
GM-502B	Y = 9.99X - 106.16	r = 0.99
GM-102B	Y = 12X - 90.88	r = 0.99
GM-302B	Y= 11.45X - 174.87	r = 0.99
GM-702B	Y = 0.97X + 765.37	r = 0.85
MQ-136	Y = -0.36X + 625.23	r= -0.29
BME-860 VOC gas sensor	Y= -6836X + 545339	r= -0.95

2.3. Data Preprocessing

In this study, four classes of smoke that are fresh air (background), cigarettes, Oud, and burning tissue smokes were used. 600 data files were acquired for each class. In addition, each data file had 20 data samples for each gas sensors. In the beginning, the collecting data samples were calibrated to be acquired at 25 °C as shown in Figure 3. after that, these collected data samples were normalized for each gas sensor using Equation (5) [17]:

$$X_{norm} = \frac{X - X_{min}}{X_{max} - X_{min}} \tag{5}$$

where X_{norm} is the normalization value, X is a sample value, X_{min} is the minimum value of the data samples, and X_{max} is the maximum value of the data samples. This normalization process improved the performance of training machine learning (ML) model by using single scale for all data samples. After doing normalization process, each data file had 20 normalized data samples for each gas sensor. Average, standard deviation, minimum, maximum, and root mean square (RMS) values were calculated for each gas sensors in the data file as shown in Figure 3. Then these values will be used to training the DNN model.

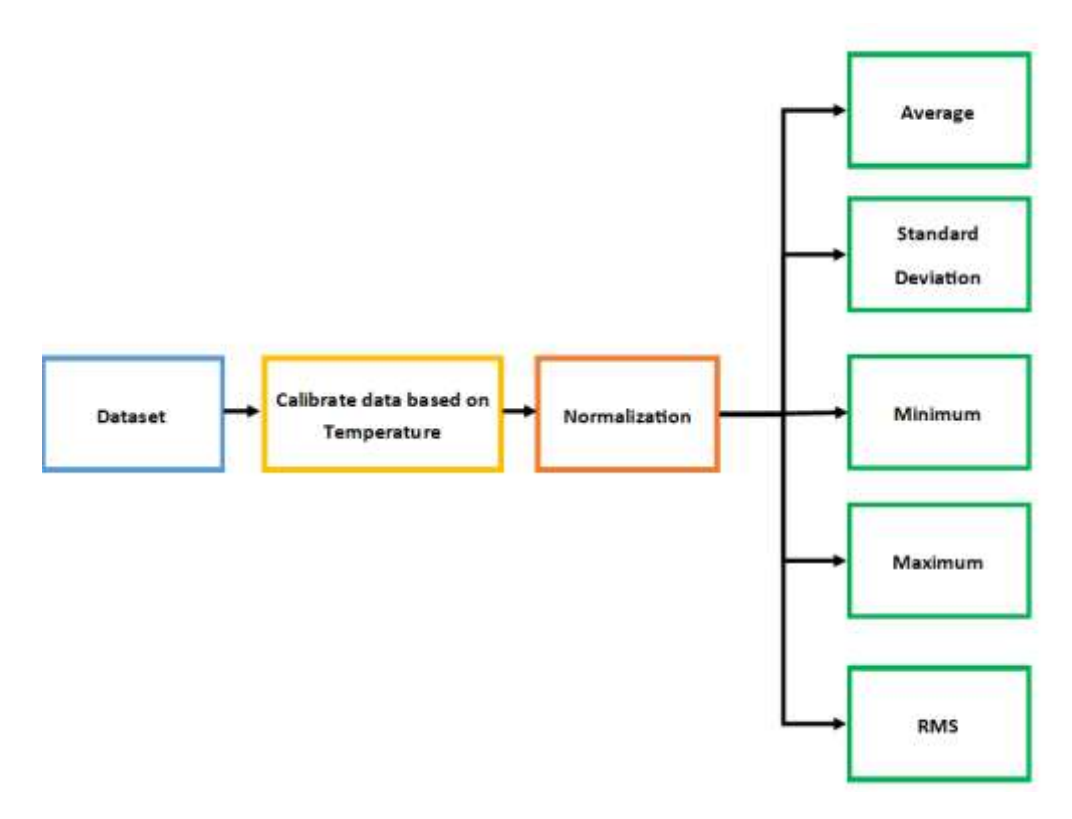


Figure 3. The steps of preprocessing data.

2.4. Deep Neural Networks (DNN) Model

TensorFlow that is an open-source deep learning software [18] was used to design and train the smoke classification model as shown in Figure 4. The input of this model is an array of preprocessing data consists of 30 elements. As a result, the input layer of DNN contain 30 nodes. In addition, this DNN has two hidden layers and one dropout layer as shown in Figure 4. The first hidden layer consists of 30 nodes while the second hidden layer had 10 nodes. The activation function of these hidden layers was rectified linear unit (ReLU) [19]. The dropout layer was also set between these two hidden layers to avoid overfitting [20]. The percentage of dropout was 20%. The output layer had 4 node that represented the classification classes. The activation function of this layer was softmax. In this training, the dataset was divided into three parts that were 60% for training, 20% for validation, and 20% for testing. The sparse_categorical_crossentropy loss function and adam optimizer with learning rate = 0.001 was used. In addition, the number of epochs and batch size were 150 and 32 respectively.

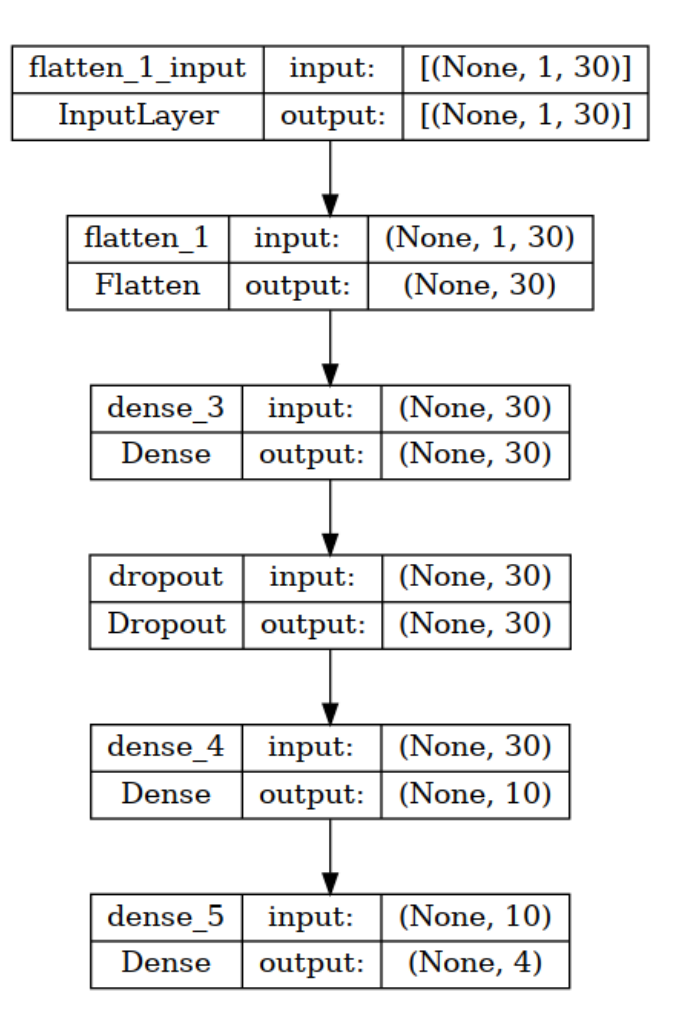


Figure 4. The structure of smoke classification model.

3. Results and Discussion

The accuracy and loss of the DNN module during training epochs is shown in Figure 5. The training and validation accuracy at epoch number 150 were 97% and 97.7% respectively. In addition, the training loss and validation loss at epoch number 150 were 0.094 and 0.052 respectively. The test accuracy of this model 97.5%. Figure 6 shows the confusion matrix for smoke classification model. This classification model predicted 100% accurate for background and cigarette smoke testing data. However, 2.7% of Oud testing data and 7.59% of tissue testing data were misclassified. The macro average precision, recall, and F1 score of the classification model were 97.48%, 97.45%, and 97.43% respectively [21].

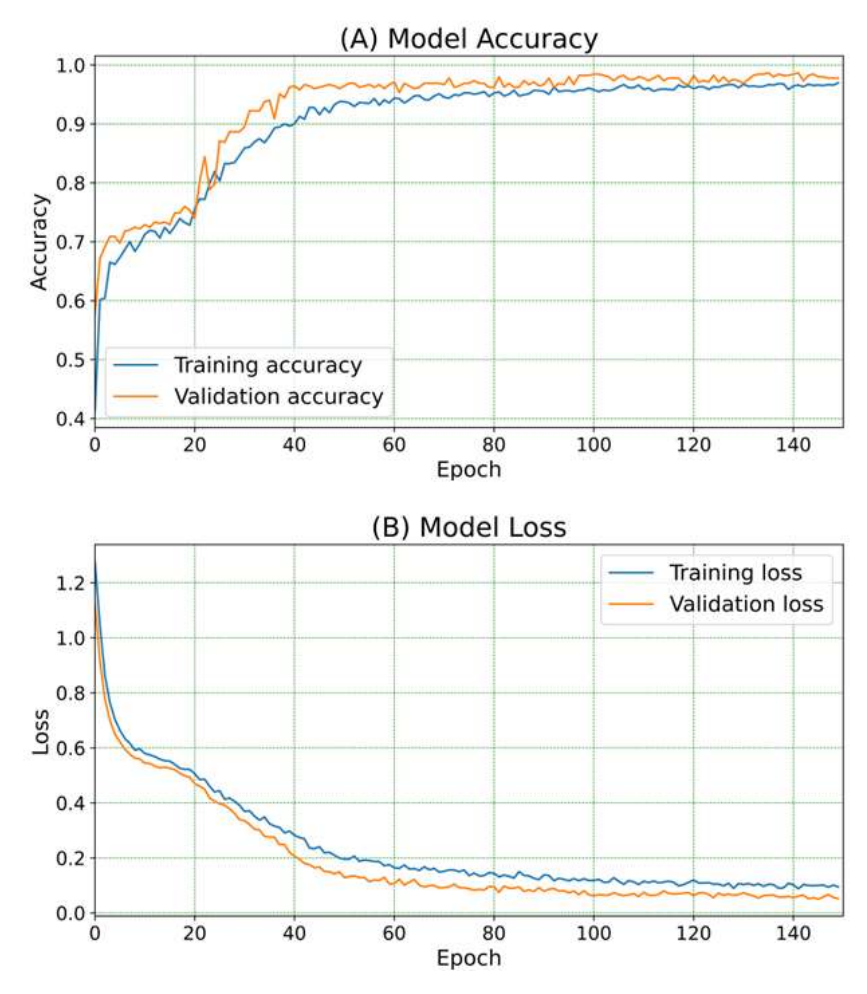


Figure 5. (A) The accuracy of DNN model, and (B) the loss of DNN model during training epochs.



Figure 6. The confusion matrix for smoke classification model.

This smoke classification model was optimized by using post training quantization technique. In this technique the model weight was quantitated from 32 bit float to 8 bit integer. This led to reducing the size, latency, and power consumption of the model. However, the accuracy of the model will be slightly reduction due to this quantization process [22]. The size of the model after applying post training quantization and converting the model to tensorflow lite (flatbuffer) was 7.4 Kbytes. Before deploying this classification model on Wio terminal, the tensorflow lite model was converted to C data file. In addition,

the Arduino tensorflow lite for microcontroller library was used to run and interpret C data file of the model.

Before providing the deployed model on Wio terminal with sensor data, these data were calibrated to be collected at 25 °C temperature. Then, these data were normalized using the maximum and minimum values of training data. After that, average, strander deviation, minimum, maximum, and RMS values for each 20 sample of each sensor were calculated to use them as an input for the model. The allocated tensor arena and inference time of the deploying model were 1.3 KB, and 226 usec respectively. This deploying model was tested in indoor environment. The temperature and humidity in the testing area were around 30 °C and 22% respectively. During the testing, the system was able to predict all smoke types. However, the prediction of the system was fluctuated for oud and tissue smokes before providing the right prediction. Based on this result, the classification smoke model can enhance the fire alarm system by providing the user with prediction of source of smoke before generating alarm signals.

4. Conclusions

In this paper, three different smoke types were classified using tiny ML technology. The accuracy of the model was 97.5%. This type of smoke classification will assist to predict the source of smoke before triggering the fire alarm system and taking action to evacuate buildings. In future work, the number of classification smoke classes will be increased. In addition, this detection system will be connected with mobile application to receive alarms and smoke sources predictions remotely.

Author Contributions: Conceptualization, A.A. (Abdulrhman Alshaya); methodology, A.A. (Abdulrhman Alshaya); software, A.A. (Abdulrhman Alshaya); validation, A.A. (Abdulrhman Alshaya); formal analysis, A.A. (Abdulrhman Alshaya); investigation, A.A. (Abdulrhman Alshaya); literature review, A.A. (Abdulrhman Alshaya) and A.A. (Abdullah Almutairi); data curation, A.A. (Abdulrhman Alshaya); writing—original draft preparation, A.A. (Abdulrhman Alshaya) and A.A. (Abdullah Almutairi); writing—review and editing, A.A. (Abdulrhman Alshaya) and A.A. (Abdullah Almutairi); visualization, A.A. (Abdulrhman Alshaya); supervision, A.A. (Abdulrhman Alshaya). All authors have read and agreed to the published version of the manuscript.

Funding: This research received no external funding.

Institutional Review Board Statement: Not applicable.

Informed Consent Statement: Not applicable.

Data Availability Statement: Data are contained within the paper.

Conflicts of Interest: The authors declare no conflict of interest.

References

- Li, X.; Vázquez-López, A.; del Río Sáez, J.S.; Wang, D.-Y. Recent Advances on Early-Stage Fire-Warning Systems: Mechanism, Performance, and Perspective. Nano-Micro Lett. 2022, 14, 197. https://doi.org/10.1007/s40820-022-00938-x.
- 2. El Barkani, M.; Benamar, N.; Talei, H.; Bagaa, M. Gas Leakage Detection Using Tiny Machine Learning. *Electronics* **2024**, *13*, 4768. https://doi.org/10.3390/electronics13234768.
- 3. Khan, M.M. Sensor-Based Gas Leakage Detector System. Eng. Proc. 2020, 2, 28. https://doi.org/10.3390/ecsa-7-08278.
- 4. Pan, G.; Xie, Y.; Yang, Q. IoT-based cloud monitoring system for building fires. *Int. J. Metrol. Qual. Eng.* **2025**, *16*, 1. https://doi.org/10.1051/ijmqe/2024020.
- 5. Sharma, A.; Khullar, V.; Kansal, I.; Chhabra, G.; Arora, P.; Popli, R.; Kumar, R. Gas Detection and Classification Using Multimodal Data Based on Federated Learning. *Sensors* **2024**, *24*, 5904. https://doi.org/10.3390/s24185904.

- 6. BME680 Low Power Gas, Pressure, Temperature & Humidity Sensor. Available online: https://www.bosch-sensortec.com/media/boschsensortec/downloads/datasheets/bst-bme680-ds001.pdf (accessed on 4 August 2025).
- 7. Grove- Multichannel Gas Sensor v2. Available online: https://docs.rs-online.com/12eb/A700000011325879.pdf (accessed on 4 August 2025).
- 8. Hydrogen Sulfide Gas Sensor (Model: MQ136). Available online: https://www.winsen-sensor.com/d/files/manual/mq136.pdf (accessed on 4 August 2025).
- 9. MEMS Carbon Monoxide Gas Sensor (Model No.: GM-702B). Available online: https://www.winsen-sensor.com/d/files/PDF/MEMS%20Gas%20Sensor/gm-702b%EF%BC%88ver1_1%EF%BC%89manual.pdf (accessed on 4 August 2025).
- 10. MEMS Alcohol Gas Sensor (Model N0.: GM-302B). Available online: https://www.cnwinsen.com/wp-content/up-loads/2021/08/MEMS-GM-302B-Manual-V1.1.pdf (accessed on 4 August 2025).
- 11. MEMS NO2 Gas Sensor (Model No.:GM-102B). Available online: https://www.cnwinsen.com/wp-content/up-loads/2021/08/MEMS-GM-102B-Manual-V2.1.pdf (accessed on 4 August 2025).
- 12. MEMS VOC Gas Sensor (Model No.:GM-502B). Available online: https://www.winsen-sensor.com/d/files/manual/gm-502b.pdf (accessed on 4 August 2025).
- 13. Wio Terminal: ATSAMD51 Core with Realtek RTL8720DN BLE 5.0 & Wi-Fi 2.4/5G Dev Board. Available online:https://mm.digi-key.com/Volume0/opasdata/d220001/medias/docus/423/102991299_Web.pdf (accessed on 4 August 2025).
- 14. Wio Terminal Tensorflow Lite Micro Getting Started. Available online: https://wiki.seeedstudio.com/Wio-Terminal-TinyML-TFLM-1/ (accessed on 4 August 2025).
- 15. How to Make an AI-Powered Artifical Nose. Available online: https://www.digikey.com/en/maker/projects/how-to-make-an-ai-powered-artificial-nose/3fcf88a89efa47a1b231c5ad2097716a (accessed on 4 August 2025).
- 16. Cantrell, C.A. Technical Note: Review of methods for linear least-squares fitting of data and application to atmospheric chemistry problems. *Atmos. Chem. Phys.* **2008**, *8*, 5477–5487. https://doi.org/10.5194/acp-8-5477-2008.
- 17. Sujon, K.M.; Hassan, R.B.; Towshi, Z.T.; Othman, M.A.; Samad, M.A.; Choi, K. When to Use Standardization and Normalization: Empirical Evidence From Machine Learning Models and XAI. *IEEE Access* **2024**, *12*, 135300–135314. https://doi.org/10.1109/AC-CESS.2024.3462434.
- 18. Syed, M.A. Overview on Open Source Machine Learning Platforms-TensorFlow. SSRN Electron. J. 2020. https://doi.org/10.2139/ssrn.3732837.
- 19. Glorot, X.; Bordes, A.; Bengio, Y. Deep Sparse Rectifier Neural Networks. In Proceedings of the Fourteenth International Conference on Artificial Intelligence and Statistics, JMLR Workshop and Conference Proceedings, June 2011; pp. 315–323. Available online:https://proceedings.mlr.press/v15/glorot11a.html (accessed on 4 August 2025).
- 20. NSrivastava; Hinton, G.; Krizhevsky, A.; Sutskever, I.; Salakhutdinov, R. Dropout: a simple way to prevent neural networks from overfitting. *J. Mach. Learn. Res.* **2014**, *15*, 1929–1958.
- 21. Takahashi, K.; Yamamoto, K.; Kuchiba, A.; Koyama, T. Confidence interval for micro-averaged F1 and macro-averaged F1 scores. *Appl. Intell.* **2022**, *52*, 4961–4972. https://doi.org/10.1007/s10489-021-02635-5.
- 22. Warden, P.; Situnayake, D. TinyML: Machine Learning with TensorFlow Lite on Arduino and Ultra-Low-Power Microcontrollers; O'Reilly Media, Inc.: Sebastopol, CA, USA, 2019.

Disclaimer/Publisher's Note: The statements, opinions and data contained in all publications are solely those of the individual author(s) and contributor(s) and not of MDPI and/or the editor(s). MDPI and/or the editor(s) disclaim responsibility for any injury to people or property resulting from any ideas, methods, instructions or products referred to in the content.